Experimental Assessment of the Effects of Cold Climate Weather Patterns on Novel PVT Collector Designs for Low Temperature Heat Pump Integration

Alonso Conejos Lopez[1], Francisco Beltran[1], Ellen Nicholson[1], Nelson Sommerfeldt[1], Valentin Delachaux[2], Mohammad Ali Jaafar[2]

[1] KTH Royal Institute of Technology, Stockholm (Sweden)

[2] DualSun, Marseille (France)

Abstract

This study investigates the impact of cold climate weather patterns on the thermal performance of two novel designs of extruded photovoltaic thermal (PVT) collectors optimized for integration with low-temperature heat pumps. The study aims to provide a comprehensive understanding of how different weather conditions, including condensation, rainfall, frost formation, and snow, affect the thermal output of these systems. The study compares two PVT designs, one with fins attached to the thermal collector and another without, to determine the optimal configuration for maximizing efficiency under varying cold climate conditions. The results indicate significant differences in performance between the finned and non-finned designs, with the finned design showing up to 11% better thermal performance. A strong impact on the thermal performance of the PVT as a result of the different weather patterns was also observed, with up to 60% thermal gains from rainfall, and 21% thermal losses during defrosting. This research fills a critical gap in the understanding of PVT performance in cold climates and provides valuable insights that can be used to determine the appropriate control strategies for heat pumps to enhance system efficiency. The findings offer a valuable contribution to the development of more efficient renewable energy systems in regions with harsh winter conditions.

Keywords: Photovoltaic thermal, solar panel, heat pump, thermal performance, climate, condensation, rain, frost, snow.

1. Introduction

Photovoltaic Thermal (PVT) panels have been a rapidly growing technology in recent years due to their ability to collect thermal energy from a photovoltaic (PV) module, thus showing increased efficiency per unit area when compared to traditional solar PV panels. This is the case for two main reasons: the heat removed from the solar panel can be subsequently used for other applications such as heating domestic hot water, and the cooling of the photovoltaic panels increases their electrical efficiency (Aste *et al.*, 2014). One of the most interesting uses for the captured heat is when the system is coupled with a heat pump, with novel PVTs designed specifically for heat pump integration being used as the sole thermal input for the system in some cases (Beltrán *et al.*, 2023).

PVT collectors for heat pump integration are of particular interest in cold climate scenarios, where the low temperature of the working fluid for the heat pump makes it possible to collect heat from the panels and the surrounding air even at times of low or zero solar irradiance. This is particularly effective with the addition of metal fins to the backside of the PVT collectors, which have been proved to enhance the thermal capture capabilities of the system (Chow, 2010). However, cold climates can exhibit unpredictable weather patterns that affect the thermal performance of the PVT system, such as condensation, rain, frost formation and snow.

Some studies in the past have explored the effects that condensation has on the efficiency of PVTs, finding overall thermal gains associated to the phenomenon (Bertram *et al.*, 2010). Other studies have also started to explore the effects of frost formation on PVT panels, but they did not focus on the defrosting process, nor the heat losses associated with the presence of an ice layer on the thermal collector surface (Chhugani *et al.*, 2020). Rain and snow, however, have not received much attention in previous research and their effects remained largely unexplored. Therefore, further research in this area will be useful to understand how these weather patterns affect the thermal performance of the PVTs. The results from this study will help to shed some light on the optimal way to operate the heat pumps in combination with the PVT modules for cold climate operation,

Selection and/or peer review under responsibility of Scientific Committee
10.18086/eurosun.2024.07.11 Available at http://proceedings.ises.org

as well as what PVT design characteristics increase thermal performance under such conditions.

2. Objectives

The objective of this study is to provide a detailed analysis of the effects of cold weather patterns on the thermal performance of two novel designs for extruded PVT collectors optimized for heat pump integration through experimental testing. The difference between the panels is a set of fins located on the thermal collector of one of the panels to increase its surface area. The experiments performed will provide a better understanding of how these two different collector designs perform in cold climate settings, as well as how big of an impact the weather patterns have on the system. Additionally, advancing the research for PVT with heat pump integration will provide an indication as to what the optimal operating parameters are in order to maximize the thermal performance of the system under such weather conditions. These objectives will be achieved by answering the following research questions:

1. How does condensation impact the thermal output of the PVTs?
2. How does rainfall impact the thermal output of the PVTs?
3. How does frost formation and defrosting impact the thermal output of the PVTs?
4. How does snow impact the thermal and electrical output of the PVTs? How much energy is required to shed the snow layer?
5. How do the finned and the non-finned PVT designs compare under these different weather conditions?

3. Methods

3.1. Test environment description

The experiments in this study were performed in an outdoor laboratory at KTH Royal Institute of Technology in Stockholm, Sweden. The system diagram for the testing equipment is shown in Fig. 1. The laboratory is equipped with a South-facing array of photovoltaic solar panels with thermal collectors attached to the back (PVTs) at an inclination of 45°. The panels are manufactured by DualSun, rated at 425W of electrical power, and have an extruded aluminium thermal collector attached to the back. The collectors are optimized for heat pump integration and use an adapted box-channel design with harp configuration, pressed mechanically to the back of the PV panel with springs. Fig. 2 shows the two collector designs, one with fins (finned) and one without (non-finned).

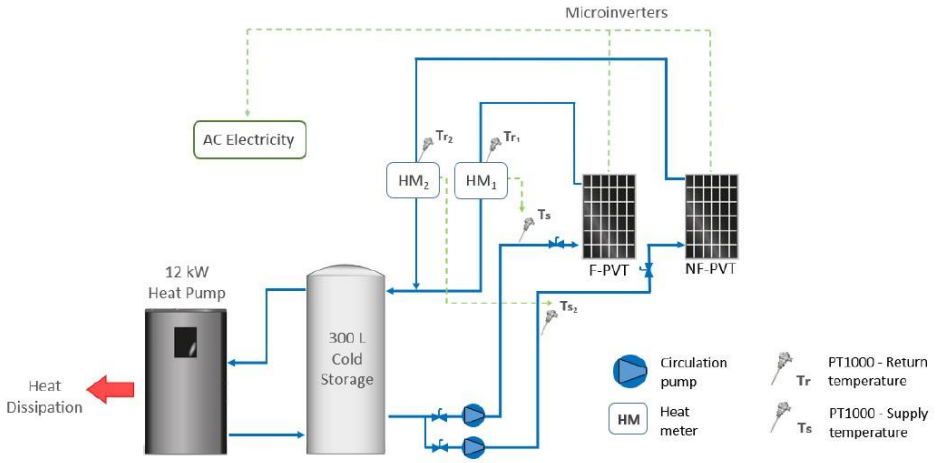

Fig. 1 Test bench system diagram.

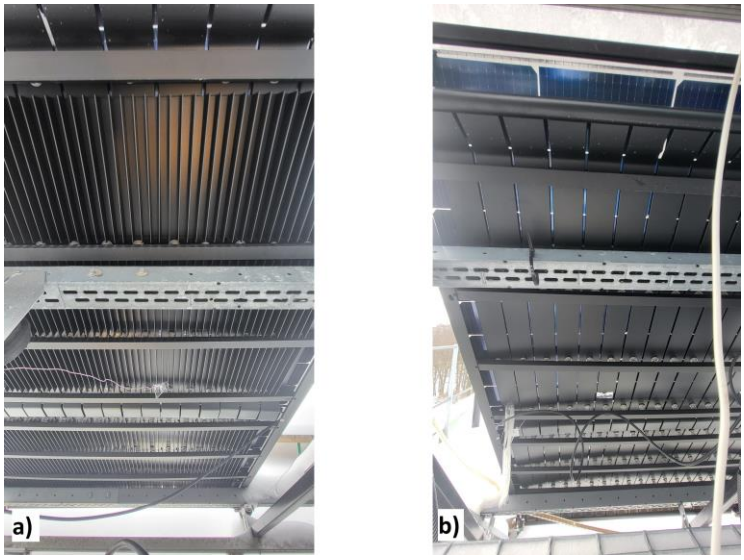

Fig. 2: a). Finned thermal collector and b). Non-finned thermal collector designs

The PVTs are connected via a set of pipes to a variable speed heat pump rated at 3-12kW (Thermia model Atlas 12 400V), which uses a mixture of ethylene glycol and water (volumetric ratio 1:3) as the working fluid and can reach temperatures as low as -10°C in the summer months. A set of LOWARA pumps circulates the fluid and allows to change the volumetric flow rate of the fluid. The panels are connected in two parallel loops, which allows for both of them to be run simultaneously and tested under the same conditions.

The system is also equipped with a variety of measuring devices that monitor the thermal performance of the system as well as the dynamic ambient conditions present at the outdoor laboratory. A set of 2Flow AB heat meters measure the thermal power generated by the PVTs and monitor the inlet and outlet temperatures of the working fluid. Additionally, a weather station located on-site provides accurate measurements on the atmospheric conditions, including ambient temperature, wind speed, wind direction, relative humidity, and dew point. A solar irradiance meter is also located next to the panels with the same tilt angle to measure the global solar irradiance in the plane of the array. Finally, eight different thermocouples can be used to measure the temperature distribution of the thermal collector during operation, or other useful measurements like the temperature of the rain.

3.2. Experiment setup

The experiments conducted in this study consist of different tests run on the PVT system with heat pump integration described in Section 3.1. during times when the PVTs were affected by condensation, rainfall, frost, or snow. A baseline model is also created during times where none of the weather patterns are present, and is used for comparison with the other experiments.

These tests are performed at normal operating conditions, unless required and stated otherwise. Normal operating conditions follow the indications from the PVT manufacturer and consist of a volumetric flow rate of 100 l/h per panel, and a PVT outlet temperature of 3 – 6 °C less than the ambient temperature. The experiments were conducted between March and May of 2024 in Stockholm, Sweden, so a range of atmospheric conditions representative of cold climates could be observed.

3.3. Data analysis

From the measurements obtained of the inlet and outlet temperature, as well as the flow rate of the working fluid, the thermal power for each panel is calculated following eq. 1:

$$\dot{q} = \frac{\frac{\dot{V}}{\rho(T_m)} c_p (T_{out} - T_{in})}{A_G} \qquad \text{(eq. 1)}$$

Where $\dot{q}$ is the specific thermal power per unit area, $\dot{V}$ is the fluid volumetric flow rate, ρ is the fluid density, T_m is the mean fluid temperature, c_p is the fluid specific heat capacity, T_{out} is the fluid temperature at the PVT outlet and T_{in} at the inlet, and A_G is the collector area.

According to the ISO standard 9806:2017, a polynomial regression can be used to model solar thermal

collectors under steady state conditions, while also considering the weather conditions (ISO, 2017). An adaptation of this formula used for this study is shown in eq. 2:

$$\dot{q} = \eta_0 G - a_1(T_m - T_a) - a_3 u(T_m - T_a) - a_6 uG \qquad \text{(eq. 2)}$$

Where η_0 is the zero loss efficiency, a_1 is the heat loss coefficient, a_3 is the wind speed dependence of the heat loss coefficient, a_6 is the wind speed dependence of the zero-loss efficiency, G is the perpendicular solar irradiance, T_a is the ambient temperature, and u is the surrounding air speed. These two equations combined are used to determine the thermal performance coefficients η_0, a_1, a_3, and a_6. These coefficients serve as a polynomial model to estimate what the thermal power should be under a different set of conditions, and a comparison between the measured and the modelled value is made. Finally, the coefficient of determination R^2 is calculated to determine how well the regression model fits the measured data, with a value of 1 being a perfect fit and 0 being no correlation between the model and measured data at all.

4. Results

4.1. Baseline model

The baseline model was created from data points collected during times where none of the weather patterns assessed in this study were present, and the data was filtered out if the conditions for condensation or frost were given, or if rain or snow were observed. The system was run at normal operating conditions during different times spanning the duration of the experimental part of the study, accumulating a total of 3408 data points (over 56 hours of cumulative data), to create a comprehensive model that could be used to compare the different patterns, as explained in section 3.3. The Baseline was divided into an overall baseline, and three cases with zero irradiance, low irradiance, and high irradiance, to better represent different moments of the day or atmospheric conditions. The thermal performance coefficients and coefficients of determination for all the baseline cases are displayed in Tab. 1. When looking at the total thermal energy produced by each type of PVT, the finned panel thermally outperformed the non-finned panel by about 6% overall, 4% for zero irradiance, 1% for low irradiance, and 8% for high irradiance.

Tab. 1: Baseline thermal performance coefficients and calculated coefficients of determination.

	Overall		**Zero Irradiance**		**Low Irradiance**		**High Irradiance**	
	Non-finned	Finned	Non-finned	Finned	Non-finned	Finned	Non-finned	Finned
η_0	0.42	0.51	0.00	0.00	0.29	0.38	0.42	0.52
a_1	38.46	34.11	37.65	36.12	45.41	39.49	36.41	29.13
a_3	3.00	4.25	2.68	4.59	0.08	2.45	4.68	5.51
a_6	0.00	0.00	0.00	0.00	0.00	0.01	0.00	0.00
R^2	0.94	0.92	0.49	0.48	0.70	0.64	0.83	0.80

4.2. Condensation

The condensation experiments were run when the atmospheric conditions allowed for the temperature at the collector surface to be below the dew point, but above freezing. When these conditions were met, the water molecules suspended in the air changed from gas to liquid phase. Fig. 3 shows the finned and non-finned panel at a time when condensation was present on the collector surface. These conditions occurred mainly in the spring months of April and May, on days of high humidity and warmer temperatures. Four separate experiments were conducted where condensation was successfully formed on the collector surface, with 4688 data points collected (over 78 hours of cumulative data after filtering). In order to maintain the conditions for as long as possible while preventing frost from forming, the fluid temperature was set to 1°C, while the volumetric flow rate was maintained at the recommended setting of 100 l/h per panel. The experiment was subdivided into times with zero irradiance (nighttime) and times with nonzero irradiance (daytime). The thermal performance coefficients and the calculated coefficients of determination are shown in the appendix in Tab. A1.

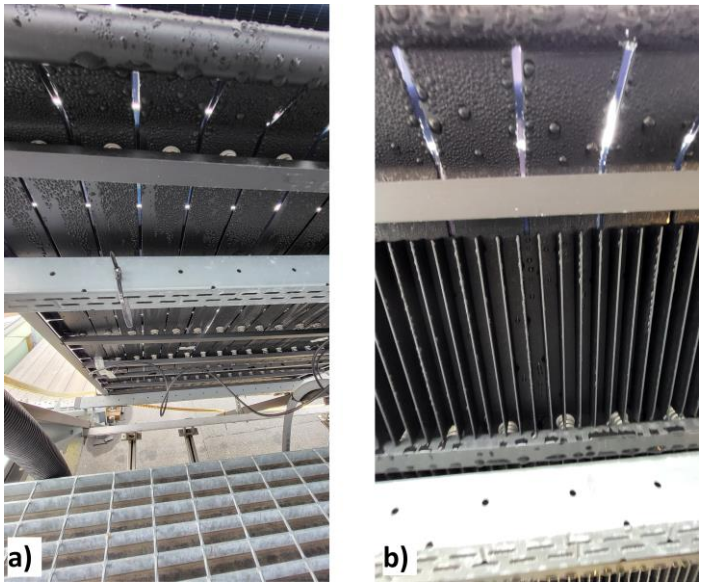

Fig. 3: Condensation forming on the collector surface for a) non-finned panel and b) finned panel.

When looking at the zero irradiance data for this experiment, the measured average specific heat output was around 3% lower than what the zero irradiance baseline model would have predicted for the same atmospheric conditions for the non-finned panel, and roughly 8% lower for the finned panel. The thermal power output of both panels was very similar, with the finned panel producing 0.5% less thermal energy than the non-finned panel.

For the nonzero irradiance data, the comparison to the baseline was made with the low irradiance baseline, as it was the one that best matched the irradiance conditions during the condensation experiments. With this comparison, the non-finned collector returned a heat losses similarly to the zero irradiance case, with a 4.4% reduction in average specific power output compared to the baseline model. However, the finned panel showed condensation gains of 1%. The finned panel also showed a small improvement in performance with respect to the non-finned panel, producing 6.3% more average specific thermal power, as well as better improvement with respect to the baseline.

4.3. Rain

The rain tests were conducted when rainfall was observed and recorded by the weather station present on-site. In addition to the power measurements, the amount of rainfall and the rain temperature were also recorded. However, the weather station was only able to measure rainfall surpassing 0.2mm per hour, so times when the rainfall amount was lower than that were discarded. Additionally, the weather station only records rainfall in 0.2mm increments, so in order to estimate the actual amount of rainfall at any given time, an average was made dividing the amount of rainfall in a specific time period by the length of said period. These experiments were conducted mainly in the spring months of April and May, accumulating 1333 data points collected (over 22 hours of cumulative data). These tests were run under normal operating conditions, and were subdivided into times with zero irradiance and times with nonzero irradiance. The thermal performance coefficients and the calculated coefficients of determination are shown in the appendix in Tab. A2. This experiment is an exception since it is not compared to the baseline model. Instead, the thermal performance coefficients from the condensation experiment are used to create a model following the same steps as for the baseline. This condensation model is used to compare the results from the rain experiment, since condensation is assumed to be present during such humid conditions as rainy weather.

For zero irradiance measurements, when comparing the heat output of the rain scenario to the regression model created from the condensation results, these experiments returned considerable heat gains. The non-finned panel showed an average specific heat output around 43% higher than the zero irradiance condensation model for the same atmospheric conditions, and the finned panel showed an increase in average specific heat of around 60% for the same case. The overall thermal power output of the finned panel is slightly higher than that of the non-finned panel, with around 10% more average specific power.

The heat gains of the measured data compared to the condensation regression with respect to rain temperature and rainfall amount are plotted in Fig. 4. During zero irradiance, times where rainfall occurred always generated heat gains, and the rain temperature was always measured to be higher than both ambient and mean operating fluid temperature. Fig. 4 a) shows that there is a positive correlation for both collector designs between higher rain temperatures and the heat gains compared to the modelled power, though the amount differs significantly between panels. When considering the amount of rainfall (Fig. 4 b), this shows a positive trend for the finned panel but a negative one for the non-finned panel.

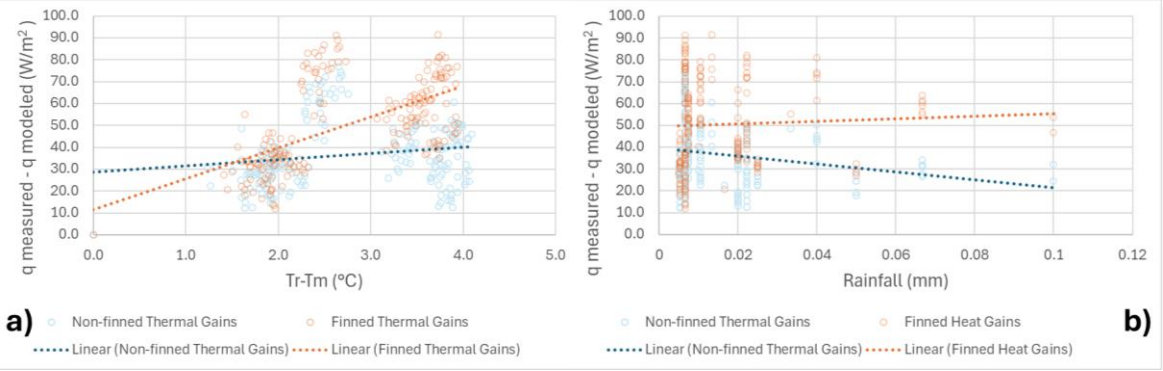

Fig. 4: Heat gains from rain compared to condensation regression during times of zero irradiance with respect to a) rain temperature, and b) rainfall amount.

For the nonzero irradiance measurements, when comparing the heat output of the rain scenario to the regression created from the condensation results, these experiments returned noticeable heat gains. The non-finned panel showed an average specific heat output around 25% higher than the nonzero irradiance condensation model for the same atmospheric conditions, and the finned panel showed gains of around 32% in the same case. These heat gains are, however, less significant than for the zero irradiance case. The overall power output of the finned panel is slightly higher than the non-finned panel, with around 7% more average specific power.

The heat gains of the measured data compared to the condensation regression with respect to rain temperature and rainfall amount are plotted in Fig. 5. During nonzero irradiance, there were times where the measured power was less than the modelled power with the condensation regression, even though the rain temperature was always measured to be higher than both ambient and mean operating fluid temperature. Results are inconsistent for both rain temperature and rainfall amount, with a weak correlation between these parameters and the heat gains, and even a slightly negative correlation in the case of rain temperature, which could be tied to the difference in $\eta 0$ coefficient for these experiments.

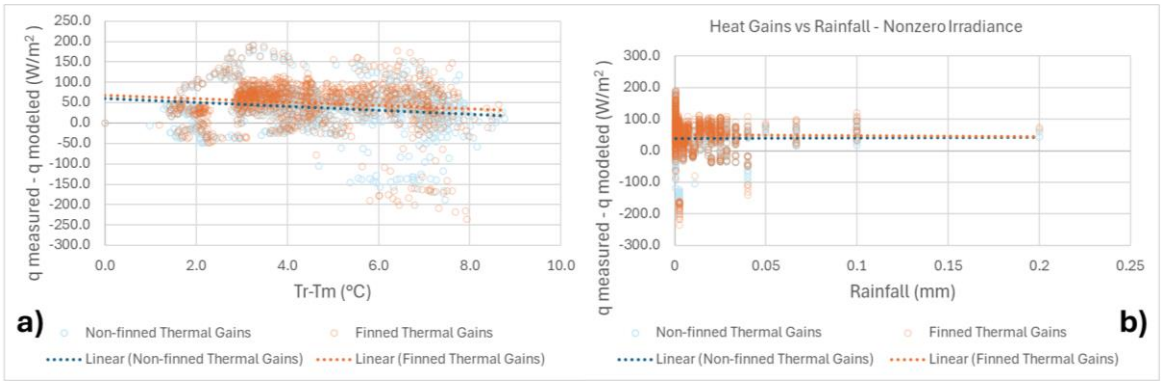

Fig. 5: Heat gains from rain compared to condensation regression during times of nonzero irradiance with respect to a) rain temperature, and b) rainfall amount.

4.4. Frost

The frost experiments were run when the atmospheric conditions allowed for the temperature at the collector surface to be below both the dew point and the freezing point. When these conditions were met, the water molecules suspended in the air changed from gas to solid phase, with some cases where the water would first condense into water droplets, then freeze. Fig. 6 shows the finned and non-finned panel at a time when frost

was present on the collector surface. These conditions occurred mainly in the late winter and early spring months of March and April, on nights of high humidity and cold temperatures. During the day, the frost then melted, and the phase change occurred in the opposite direction. Six separate experiments were conducted where frost was successfully formed on the collector surface with 4688 data points (over 102 hours of cumulative data).

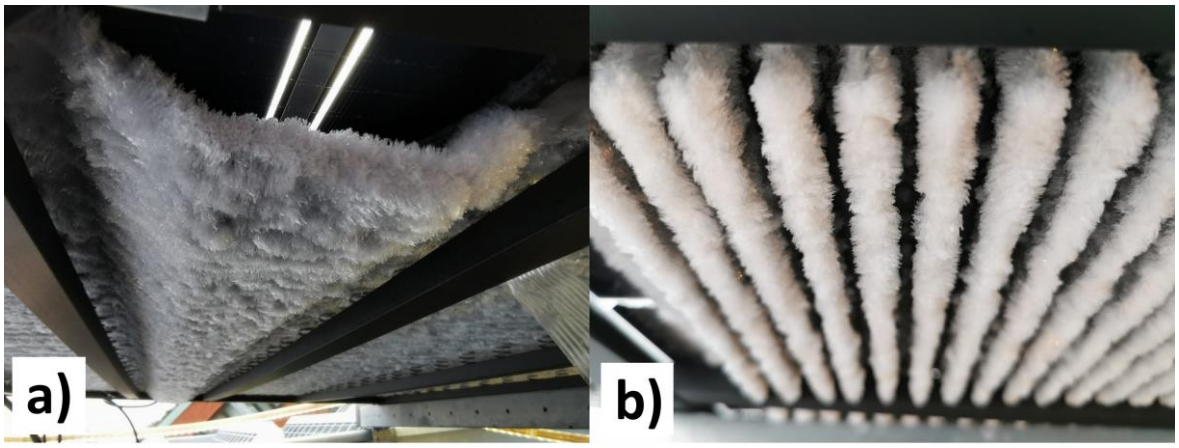

Fig. 6: Frost formation on the collector surface for a) non-finned panel and b) finned panel.

In order to maintain the frost formation conditions throughout the night, the fluid temperature was set to the minimum allowed (fluctuating between -9 to -6°C), while the volumetric flow rate was maintained at the recommended setting of 100 l/h per panel. After the sun came out and the temperature started to rise, the system was returned to normal operating conditions to allow for defrosting. The experiment was subdivided into times when frost was being formed, times when frost was present and had covered the full collector surface, and times when the panel was being defrosted. A camera was set up at the back of the finned PVT collector to monitor the different stages of the cycle. The thermal performance coefficients and the calculated coefficients of determination are shown in the appendix in Tab. A3. A comparison between the measured and modelled power for the finned panel during one of the experiments is seen in Fig. 7, outlining the different stages of the frost formation process. Both panels showed similar trends throughout all the frost experiments.

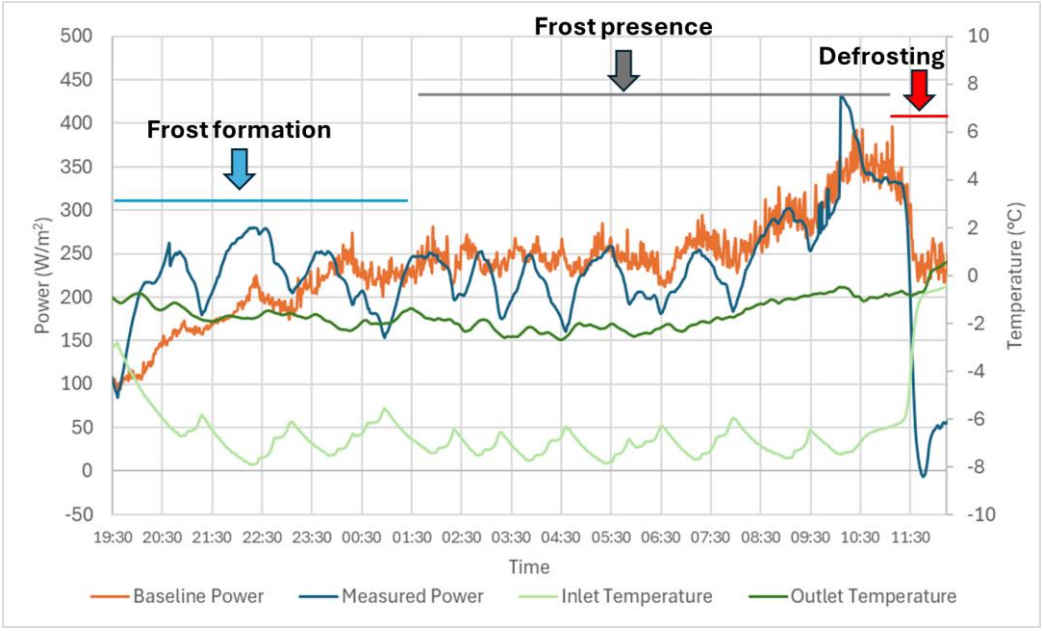

Fig. 7: Measured vs. baseline power over time for a frost formation experiment, finned collector.

When comparing the heat output of the frost formation stage to the zero irradiance baseline regression (frost formation occurred only at night), both collector designs showed heat gains of about 6%. During these times, the baseline model underestimates the power produced by the PVT, as shown in Fig.7. The overall power output of the finned panel is slightly higher than that of the non-finned panel, with around 6% more average

specific power.

For the comparison between the heat output of the frost presence stage and the overall baseline regression, both collectors showed a decline in specific thermal power, with around 18% for the non-finned panel and 15% for the finned panel. During these times, the baseline model overestimates the power produced by the PVT, as shown in Fig.7. The overall power output of the finned panel was slightly higher than the non-finned panel, with around 3% more average specific power.

Comparing the heat output of the defrosting stage to the overall baseline regression, both collectors showed a thermal performance decline, with a 21% decrease for the non-finned panel and 16% for the finned panel. During these times, the baseline model greatly overestimates the power produced by the PVT, as shown in Fig.7. The overall power output of the finned panel is noticeably higher than the non-finned panel, with around 7% more average specific power.

Additionally, a different experiment was conducted to test how different amounts of frost affected the thermal performance of the panel. The system was left running at the minimum temperature setting and an increased flow rate for over 48h until a substantial layer of frost was formed. A sample time from the start of the experiment, when the frost layer was thin, was compared to a time from near the end of the experiment, when the layer was considerably thicker. The results show that both collectors exhibit a thermal performance decline, with a decrease of about 33% for the non-finned panel and 51% for the finned panel at the end of the experiment. During this time frame at the end of the experiment the finned panel also produced around 9% less average specific thermal power than the non-finned panel. Finally, the system was returned to normal operating conditions (with the higher amount of frost still present) and compared against the baseline. Comparing the heat output of this part of the experiment to the overall baseline regression, both collectors showed a significant thermal performance decline, with a decrease in thermal power of about 43% for the non-finned panel and 34% for the finned panel. The overall power output of the finned panel is noticeably higher than the non-finned panel, with around 11% more average specific power.

4.5. Snow

The conditions for studying the impact of snow on the performance of the PVT were only given once during the experimental phase of this study, in the month of March, where a snow layer fully covered the front side of the panels and was allowed to shed naturally, as shown in Fig. 8. This test was run under normal operating conditions, and observed the time after the snowstorm stopped, until the snow layer was shed. Since only one camera was available to record the process and the shedding happened at different times for both panels, only the finned panel is observed for this experiment.

Fig. 8: Snow shedding process on the front side of the finned panel showing a) full snow cover, b) shedding start, and c) shedding end.

The layer of snow impacts both the thermal performance of the PVT, as some of the heat collected is directed towards shedding, and the electrical performance of the panel, since the sunlight is kept from reaching the surface of the panel by the layer of snow. The measured thermal power when compared to the overall baseline model returned losses of about 61%, equating to 1.12 kWh for the duration of the shedding process. In terms of electrical production, the panel produced only 123 Wh for the time frame of the experiment, while it was calculated that the panel should have produced 1141 Wh under the environmental conditions present during the test, had it been clean, which translates to an 89% reduction in electricity production. The timeline comparing measured and modelled electrical production is shown in Fig. 9, and the moments when the shedding starts at 12.30, and when it is mostly shed at 15.15 can be seen as spikes in the measured power line.

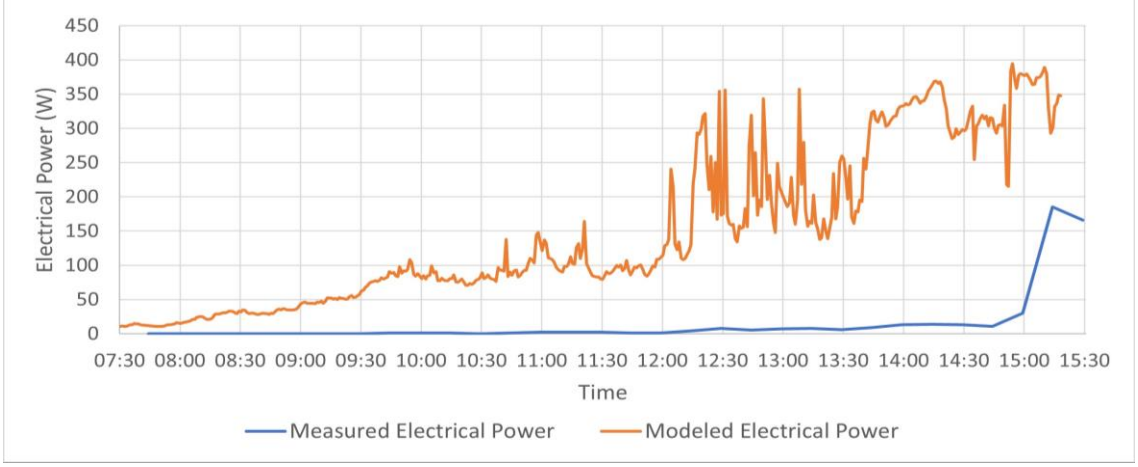

Fig. 9: Measured electrical power vs. modeled electrical power during snow shedding process.

5. Discussion

5.1. Baseline

The results obtained in this study are interesting for many reasons. In part, new findings on the effects of previously unexplored weather patterns like rain, snow, and even expanding the previous work done on frost formation serve to better understand how PVTs behave under these conditions. On the other hand, some of the expected results for previously explored phenomena like condensation formation do not match with those obtained in this study. This mismatch in the results might be caused by the way the baseline scenario was developed. The baseline is curated with a data set that has a much lower temperature difference between the ambient and the operating fluid than the other tests, following the specified guidelines for normal operation of the heat pump, while the different weather pattern experiments often operate outside of these conditions. As a result, it is possible that the baseline overestimates the heat loss coefficient $a1$, thus producing higher results in modelled power than expected when applied to situations when a much higher temperature difference is present. As a result, a direct numerical comparison between the baseline and the other experiments is inherently flawed, and these should be taken only as reference to observe trends.

The baseline did, however, provide useful information on the comparison between the finned and non-finned panel during normal operation, showing that the finned panel outperforms the non-finned panel, as is the case in most cases throughout the different experiments. However, the difference in average thermal output is not always as significant as one could expect, particularly for the low irradiance baseline scenario, where the finned panel only has a 1% increased thermal output. The finned panel is also more susceptible to effects of atmospheric conditions, showing higher dependence on the wind speed and irradiance levels than the non-finned panel.

5.2. Condensation

The condensation experiments returned surprising results, with this phenomenon netting thermal losses with respect to the baseline. From previous research, and following the laws of physics, it would be expected that condensation nets heat gains related to the phase change from gas to liquid (Betram *et al.*, 2010). The energy released during the phase change could be captured by the collector, and since the surface is slanted, the water droplets just slide off the panel, so the phase change is unidirectional. This difference in the results obtained could be due to the way the results are compared to the baseline, as explained previously. Looking at both panels, however, the finned panel does generally perform better than the non-finned panel as expected, which agrees with the results obtained by Chhugani *et al.* (2020).

5.3. Rain

The results from the rain experiment return the highest thermal gains among all, with up to 60% gains for the

finned panel during nighttime operation, which is to be expected since the rain temperature was measured to be higher than both ambient and fluid temperature at all times. The finned panel once again outperforms the non-finned panel for these experiments, being able to better take advantage of the warmer, more humid surrounding air. Regarding rainfall amount and rain temperature, it would be expected that higher values of both rainfall and temperature difference would net higher gains. However, only the rain temperature dependence of the zero irradiance case shows a clearly positive correlation. When the nonzero irradiance cases are observed, there seems to be no clear correlation between these parameters and the calculated thermal gains. A possible explanation is that once the system reaches a steady state, the rain has already incresed the output fluid temperature, and thus the average temperature of the working fluid, reducing the difference between rain temperature and mean fluid temperature, (X-axis in Fig. 4 and 5). Therefore, the highest thermal gains recorded, when the inlet and outlet fluid temperature difference is highest, correspond to moments when the mean fluid temperature has already risen, while the highest difference between rain temperature and mean operating fluid temperature will happen right at the start of rainfall, before the rain has affected the outlet fluid temperature and the system is not yet in steady state. With regards to rainfall amount, it is possible that a small amount of rainfall is enough to get the front side of the panel to match the rain temperature, therefore saturating as rainfall increases, which could explain the mostly flat trend lines when looking at heat gains in terms of rainfall amount.

An interesting observation is that the highest losses measured corresponded to times of higher measured irradiance. This could be due to the fact that the rain might be cooling down the panel, thus limiting the effect of the irradiance. This hypothesis is supported by the fact that the $\eta 0$ coefficient is almost 0 for the nonzero irradiance cases in the rain experiments, and up to 0.5 for the condensation regression. This is consistent with the explanation that a small amount of rainfall is enough to change the temperature of the front side of the panel. Regardless, it is clear that rain heat gains compared to the condensation scenarios are highest for cases with no irradiance, and are worst at cases with higher irradiance, where the effect of the rain and the sun are arguably counteracting each other.

5.4. Frost

Similarly to the condensation experiment, this scenario expects heat gains associated with the phase change from gas to solid as the water molecules in the air freeze onto the collector surface. This is supported by the early stages of the frost formation cycle, where heat gains are observed. However, during defrosting the phase change occurs in the other direction, and heat losses are sustained. However, there is only one phase change occurring in this stage since the water goes from solid to liquid, and then proceeds to drip off the panel. During the time the panel is fully covered until it starts to defrost, the results also show associated losses compared to the model. This could be the case because a layer of frost limits the heat exchange with the surrounding air. This hypothesis is further supported by the experiment where different layers of frost were compared, and a thicker layer of frost was found to have reduced performance compared to a thinner layer. Additionally, since the frost presence shows to negatively impact the thermal performance of the system, the longer this state is held, the more the overall thermal production through for the whole cycle.

In this experiment the finned panel once again outperformed the non-finned panel during the normal frost cycles, which is to be expected as a larger surface area leads to more frost forming on the collector. However, this can turn out to be a disadvantage, as the finned collector performed worse than the non-finned one while the thick layer of frost was present.

5.5. Snow

This experiment on the impact of snow showed how detrimental a snow layer can be to the overall performance of a PVT system, since it impacts not only the thermal performance but also the electricity production. Previous research on snow and PVTs focused on whether it is possible to actively shed the layer of snow from the panel by running the heat pump in reverse (Rahmatmand *et al.*, 2019). However, the system used for this study did not have that capability. Instead, the snow layer was allowed to shed naturally, and the thermal losses sustained during that period of time were assumed to be directed to melting the snow and the shedding process. Therefore, if the amount of energy required to actively shed the panel were the same as the losses associated with passive shedding (1.12 kWh), it would not be energy efficient to actively shed the panel in this case, since the expected electrical gains from doing so (1.02 kWh) would not cover the energy needed for the process.

Perhaps turning off the system until the snow has fully shed would be optimal.

6. Conclusion

The results from this study show that there is indeed a considerable impact from cold climate weather patterns on the thermal performance of PVTs. While condensation was expected to provide thermal gains as found in previous research, the opposite occurred for the experiments conducted in this study. Rain was the phenomenon with the highest calculated thermal gains, as the rain temperature was consistently above ambient, thus warming the panels. However, it seems that just a small amount of rainfall is enough to get a positive effect on thermal performance, and higher amounts of rainfall have diminishing returns. Frost formation showed varying results depending on the stage of the cycle: while the formation of frost generates some thermal gains, the defrosting stage and the presence of frost on the collector surface have detrimental effects on the thermal performance of the system. Finally, snow returned considerable energetic losses for both the thermal and electrical output of the system and, under the conditions experienced during the experiment, it is estimated that actively shedding the panel of the snow layer would not be energy efficient.

Comparing the finned and the non-finned PVT designs, the finned design showed better thermal performance than the non-finned design in almost every scenario. However, the difference in performance might not always be worth the extra steps during manufacturing, the heavier weight of the panel, or the increased cost. Additionally, the higher dependency on weather conditions of the finned panel lead to stronger negative effects in some of the scenarios that were tested, such as when a thick layer of frost was present.

Lastly, further work on this project would prove useful to improve the quality of the baseline and provide better comparisons, as well as to develop a more comprehensive database of all the weather patterns. It would also be beneficial to use the results obtained in this study to explore new parameters and control strategies for the heat pump to find the optimal mode of operation to increase the energy efficiency of the system when used in cold climates that present conditions such as the ones explored in this study.

7. Acknowledgments

This study was carried out under the project *Smart Renovation Strategies for Sustainable Electrification* (Project No. P2023-01509), funded by the Swedish Energy Agency (Energimyndigheten) as part of the ReBygg Program.

Special thanks to the people from the KTH department of Energy Technology, and to the project partner DualSun, who provided the PVTs used for the study.

8. References

Aste, N. del Pero, C. and Leonforte, F. (2014) 'Water flat plate PV–thermal collectors: A review', Solar Energy, 102, pp. 98–115. Available at: https://doi.org/10.1016/j.solener.2014.01.025.

Beltrán, F., Sommerfeldt, N. and Madani, H. (2023) 'Experimental testing of solar photovoltaic/thermal collector as a heat pump source under outdoor laboratory conditions.'

Bertram, E. Scheuren, J. Glembin, J. and Rockendorf, G. (2010) 'Condensation heat gains on unglazed solar collectors in heat pump systems,' pp. 1–8. 10.18086/eurosun.2010.07.02.

Chhugani, B. et al. (2020) 'Model Validation and Performance Assessment of Unglazed Photovoltaic-Thermal Collectors with Heat Pump Systems', in. Available at: https://doi.org/10.18086/eurosun.2020.05.13.

Chow, T.T. (2010) 'A review on photovoltaic/thermal hybrid solar technology', Applied Energy, 87(2), pp. 365–379. Available at: https://doi.org/10.1016/j.apenergy.2009.06.037.

ISO, (2017). ISO9806: Solar Energy – Solar Thermal Collectors -Test Methods.

Rahmatmand, A. Harrison, S. J. and Oosthuizen, P. H. (2019) 'Evaluation of removing snow and ice from photovoltaic-thermal (pv/t) panels by circulating hot water,' Solar Energy, vol. 179, pp. 226–235. Available at: https://doi.org/10.1016/j.solener.2018.12.053.

9. Appendix

9.1. Condensation

Tab. A1: Condensation thermal performance coefficients and calculated coefficients of determination.

	Zero Irradiance		**Nonzero Irradiance**	
	Non-finned	Finned	Non-finned	Finned
η_0	0.00	0.00	0.47	0.50
a_1	37.13	37.07	24.43	22.37
a_3	1.60	1.69	6.70	8.93
a_6	0.00	0.00	0.06	0.08
R^2	0.78	0.78	0.79	0.78

9.2. Rain

Tab. A2: Rain thermal performance coefficients and calculated coefficients of determination.

	Zero Irradiance		**Nonzero Irradiance**	
	Non-finned	Finned	Non-finned	Finned
η_0	0.00	0.00	0.02	0.00
a_1	51.71	57.45	45.52	48.95
a_3	1.63	2.71	5.09	6.43
a_6	0.00	0.00	0.00	0.00
R^2	0.94	0.94	0.89	0.87

9.3. Frost

Tab. A3: Frost thermal performance coefficients and calculated coefficients of determination.

	Frost formation		**Frost Presence**		**Defrosting**	
	Non-finned	Finned	Non-finned	Finned	Non-finned	Finned
η_0	0.00	0.00	0.00	0.00	0.04	0.00
a_1	41.71	44.00	34.42	33.10	33.42	35.92
a_3	1.16	2.12	1.86	4.18	3.95	4.64
a_6	0.00	0.00	0.00	0.00	0.02	0.00
R^2	0.82	0.81	0.83	0.81	0.94	0.90